



EMC/EMI Issues in Biomedical Research

Ji Chen

Department of Electrical and Computer Engineering

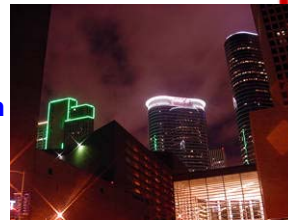
University of Houston

Houston, TX 77204

Email: jchen18@uh.edu



UH: close to downtown of Houston
35,066 students



ECE Department: 35 faculty members, 250 graduate students

Electromagnetic Research at University of Houston:

NSF Center For Electromagnetic Compatibility Research

Areas:

Computational Electromagnetics

Antennas

High-Speed Signal Propagation

Bioelectromagnetics

Nano-devices

Wireless Propagation

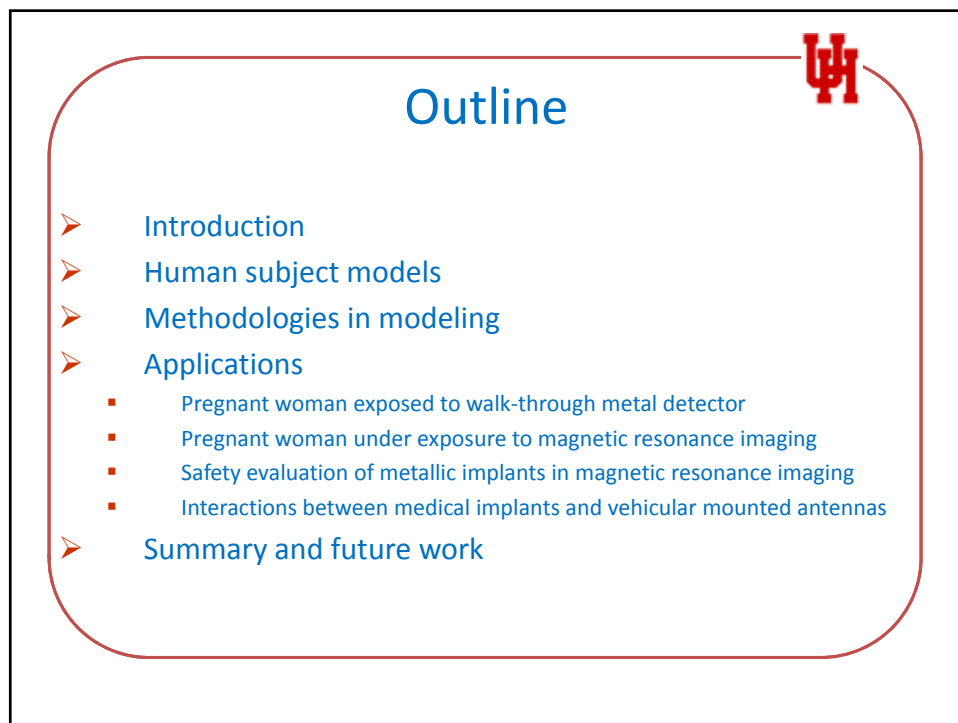
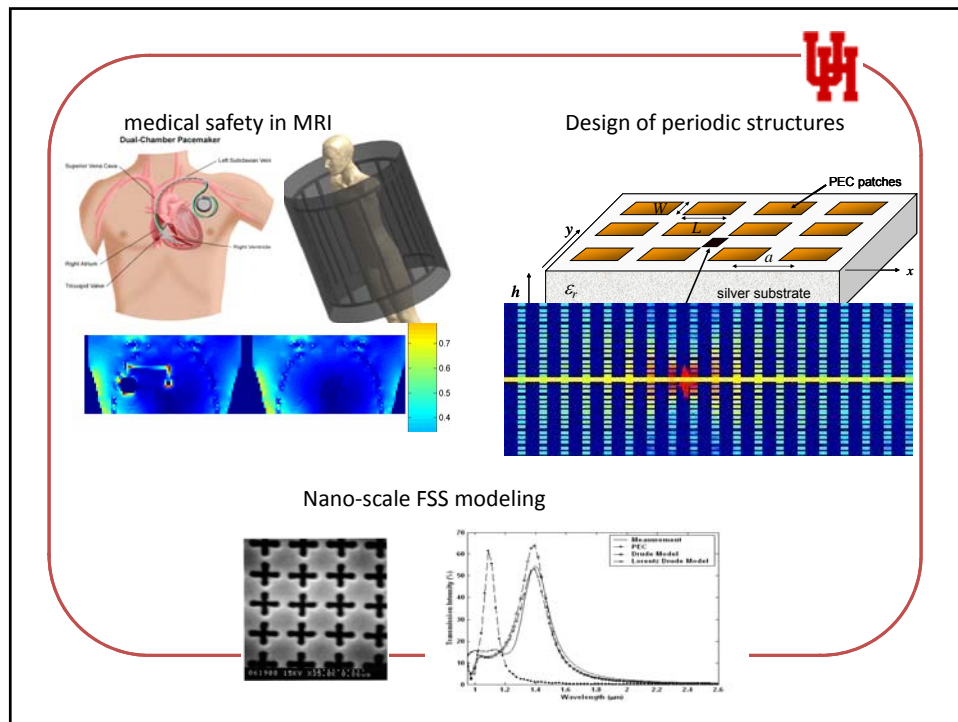
Faculty Members:

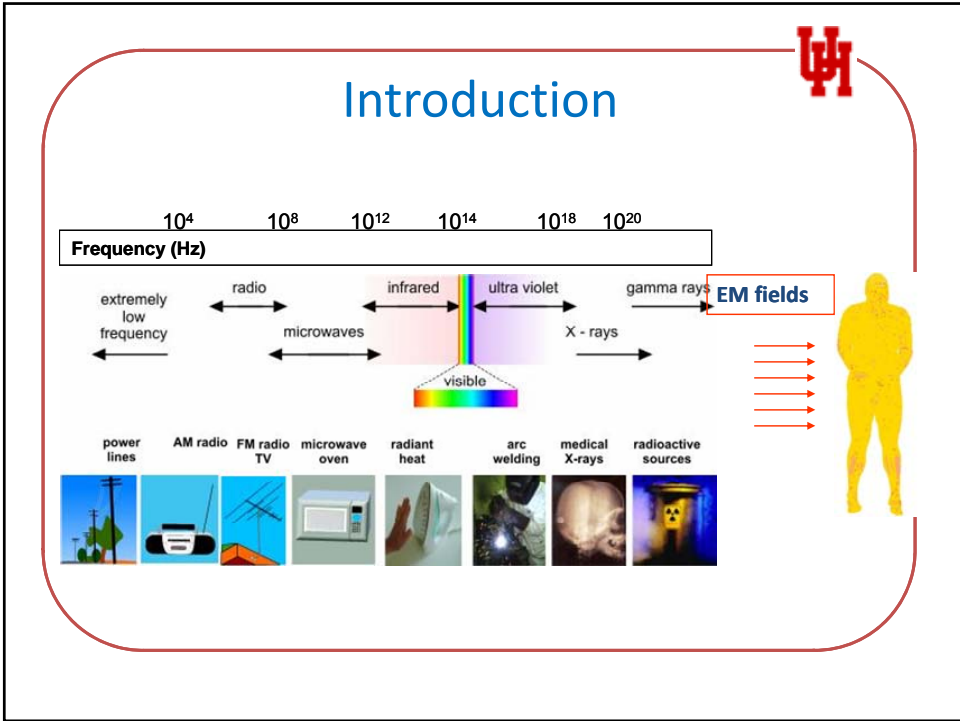
6 faculty members

IEEE Board of Directors

past president of AP society

4 IEEE Fellows






Magnetic stimulation in human head (low frequency)

- severe [depression](#)
- auditory [hallucinations](#)
- migraine headaches
- [tinnitus](#)

Magnetic resonance imaging (radio frequency)

visualize the inside of living organisms


6



A head-to-toe uniform detection field

Pinpoint Detection with DSP Chip


The slide features a red rounded rectangle containing a diagram of a person walking through a blue metal detector frame. Red dashed arrows point from the frame to a photograph of a person standing in a metal detector. The Psi logo is in the top right corner.



•The problem of human exposure to high/low frequency electromagnetic fields has been the subject of many studies.

- Electromagnetic and temperature analysis of [high-frequency exposure](#)
 - SAR (energy deposition)
 - Temperature (thermal distribution)

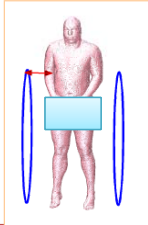

EM fields → Energy deposition → Tissue heating



•Calculate induced current density and induced electric field in human body due to [extremely-low-frequency exposure](#)

- J (current density) & E (electric field)

EM fields → Induced current

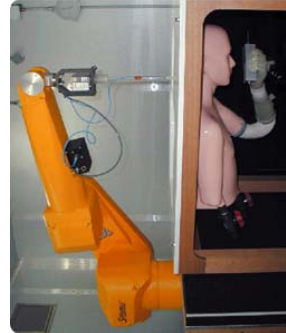
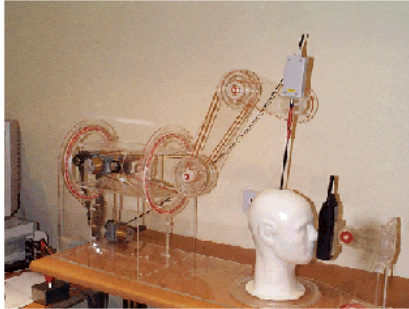


Anti theft device model

The slide features a red rounded rectangle containing text, flowcharts, and images. The Psi logo is in the top right corner. The flowcharts show the relationship between EM fields, energy deposition, tissue heating, induced current, and an anti-theft device model.



Approach 1: Experimental measurement



disadvantages:

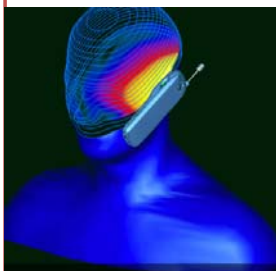
- I. difficult to make models.
- II. filling material is homogeneous.
- III. difficult to make measurement equipments for various EM exposure.

9

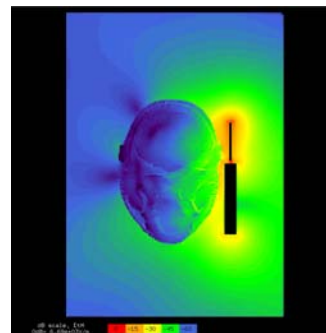


Approach 2: Numerical simulation

CAD model
+ external EM source



Numerical
method



advantages:

- I. easy to make CAD models (difficult to make for experiments).
- II. able to analyze inhomogeneous models
- III. easy to model various external EM fields.

10

Human Subject Models

Models

This slide displays various human subject models. On the left, there are three vertical anatomical diagrams: a full-body view with internal organs highlighted in red and green, a similar view with a blue background, and a smaller version. In the center, a 6-month pregnancy progression is shown with eight images labeled 'Month 1' through 'Month 6'. To the right, there is a 3D head scan with a color gradient from green to red, and a 3D skeleton model with blue and red highlights on the ribcage and spine. A red 'UP' logo is in the top right corner.

Virtual Family Models

This slide shows four virtual human models of different sizes, representing a family. Each model has a set of coordinate axes (x, y, z) overlaid on its body. The models are arranged from largest to smallest from left to right. A red 'UP' logo is in the top right corner.

Tissue parameters

Dielectric & thermal properties

CAD Model (including different internal organs/tissues)

↓

Assign tissue parameters for each internal organs/tissues

↓

Final model (realistic human body)

↓

Numerical simulation

Tissue	ρ [kg/m ³]	64 MHz		128 MHz	
		σ [S/m]	ϵ_r	σ [S/m]	ϵ_r
Body	1006	0.49	52.54	0.51	46.23
Placenta	1058	0.95	86.50	1.00	73.19
Embryonic Fluid	1055	1.50	69.13	1.51	69.06
Bladder	1055	0.29	24.59	0.30	21.86
Bone	1990	0.06	16.69	0.067	14.72
Fetus	987	0.39	42.68	0.412	37.60
Uterus	1052	0.91	92.19	0.961	75.47


Tissue	C	K	B ₀	A ₀
	[J/kg°C]	[W/m°C]	[W/m³°C]	[W/m²]
Body	3270	0.43	2400	537
Placenta	3840	0.50	0	0
Embryonic Fluid	3840	0.50	0	0
Bladder	3300	0.43	9000	1600
Bone	1260	0.40	3300	610
Fetus	3105	0.39	2250	461
Uterus	3430	0.51	6000	1075

13

Modeling Techniques

- Low frequency bio-electromagnetic modeling
 - Impedance method → Induced current & electric fields
- High frequency bio-electromagnetic modeling
 - Finite difference time domain (FDTD) method → Specific absorption rate
- Thermal modeling in bio-electromagnetic
 - Finite difference solution of bio-heat equation → Temperature distribution
- Equivalent source → Generate required magnetic fields for impedance method

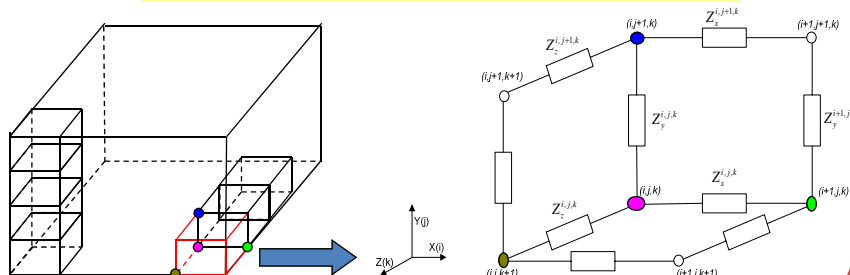
14



Method1: Impedance method


- Impedance method
 - Efficient for ELF calculation
 - Easy to implement

Equivalent circuit network for impedance method

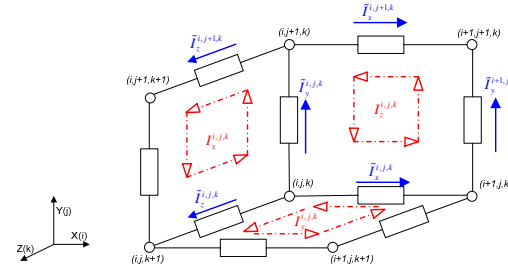


$$Z_x = \frac{\Delta x}{\Delta y \Delta z (\sigma_x + j\omega \epsilon_x)}$$

15



Impedance method



Kirchhoff voltage equations

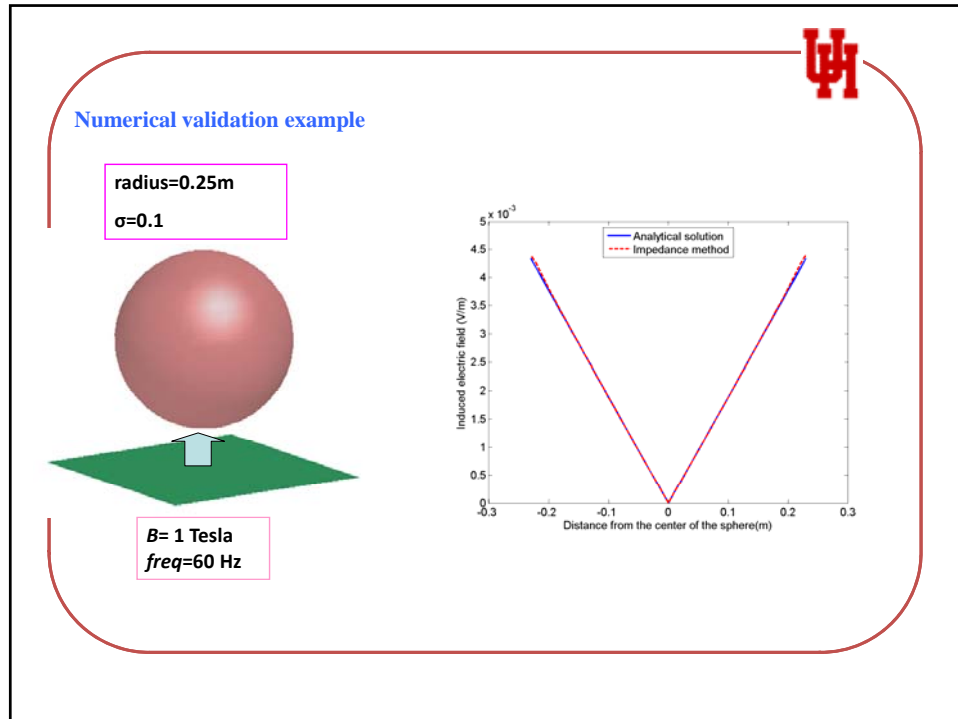
$$\sum \tilde{I}Z + j\omega\mu_0 H \square \hat{n} = V$$


$$Z_x^{i,j,k} \tilde{I}_x^{i,j,k} + Z_y^{i+1,j,k} \tilde{I}_y^{i+1,j,k} - Z_x^{i,j+1,k} \tilde{I}_x^{i,j+1,k} - Z_y^{i,j,k} \tilde{I}_y^{i,j,k} = emf_z^{i,j,k}$$

$$emf = -\frac{\partial}{\partial t} \iint \vec{B} \cdot d\vec{s}$$

$$\tilde{I}_z^{i,j,k} = I_x^{i,j,k} + I_y^{i+1,j,k} - I_x^{i,j+1,k} - I_y^{i,j,k}$$

$$\sum_{n=1}^3 a_{mn}^{i,j,k} I_n(t, j, k) = emf_m; 1 \leq m \leq 3$$





Method 2: FDTD

Modeling of interaction of electromagnetic fields with human bodies at high frequency

↓ SAR (energy deposition)


Efficient numerical technique to solve electromagnetic wave problems

$$\frac{\partial \vec{H}}{\partial t} = -\frac{1}{\mu} \nabla \times \vec{E} - \frac{\rho'}{\mu} \vec{H}$$

$$\frac{\partial \vec{E}}{\partial t} = \frac{1}{\epsilon} \nabla \times \vec{H} - \frac{\sigma}{\epsilon} \vec{E}$$

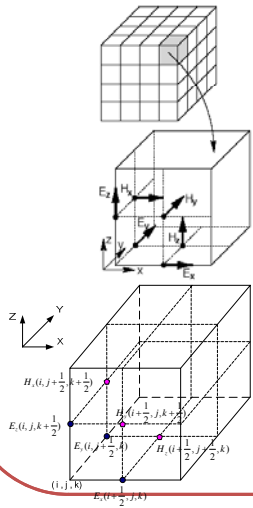
- **Finite Difference Time Domain Method**
 - Direct solution method for **Maxwell's** time dependent curl equations
 - Avoids solving simultaneous equations -- matrix inversion
 - Provides for complexities of structure shape and material composition
 - Very easy to implement compared to FEM/MOM method

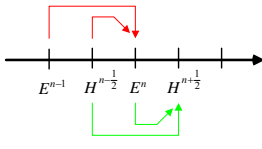
18



Method2: FDTD

Yee's FDTD Scheme






Explicit update scheme

- Easy to implement
- Able to be parallelized

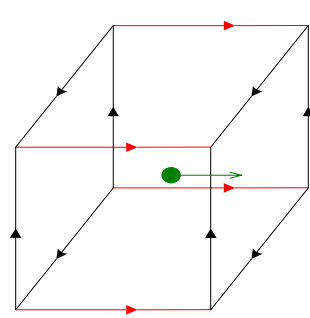
19



Method2: FDTD

Specific absorption rate (SAR) calculation


$$SAR = \frac{\sigma |E|^2}{2\rho} = \frac{\sigma (|E_x|^2 + |E_y|^2 + |E_z|^2)}{2\rho}$$



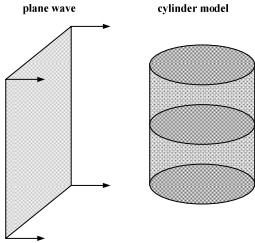
12-field components approach

$$E_{x_center_i,j,k} = \frac{E_{x_i,j,k} + E_{x_i,j+1,k} + E_{x_i,j,k+1} + E_{x_i,j+1,k+1}}{4}$$

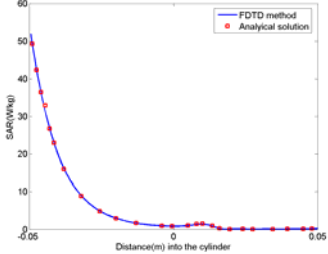
20



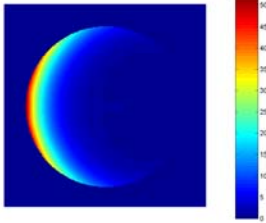
Method 2: FDTD




plane wave cylinder model



Symbol	Physical Property	Value	Units
r	cylinder radius	0.05	m
P	plane wave incident power density	1000	W/m ²
f	plane wave frequency	2.45	GHz
ϵ	relative permittivity	47	-----
σ	conductivity	2.21	S/m
ρ	mass density	1070	Kg/m ³
Δx	spatial resolution	0.5	mm



21



Method 3: Thermal modeling

- **Thermal modeling/bio-heat equation**
Temperature-rise computation
 When a human subject in a thermal equilibrium state is exposed to EM fields, the resultant temperature rises may be obtained from thermal modeling (bio-heat equation), which takes into account such heat exchange mechanisms as heat conduction, blood flow, and EM heating.

Bioheat transfer equation (BHTE):

$$C\rho \frac{\partial T}{\partial t} = K\nabla^2 T + A_0 - B(T - T_b) + Q_{EM}$$

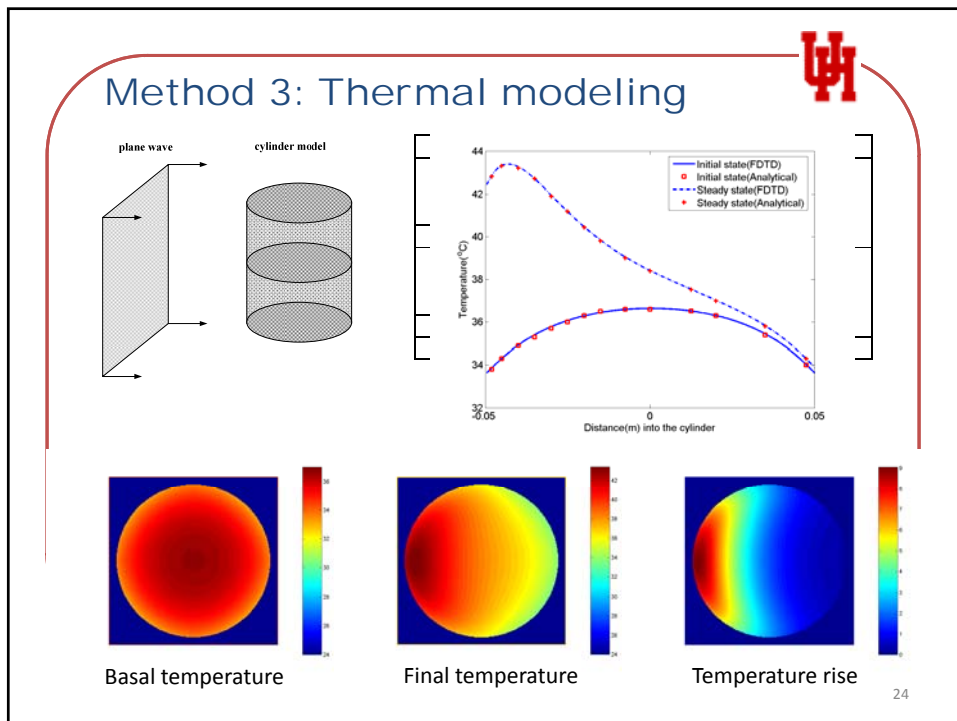
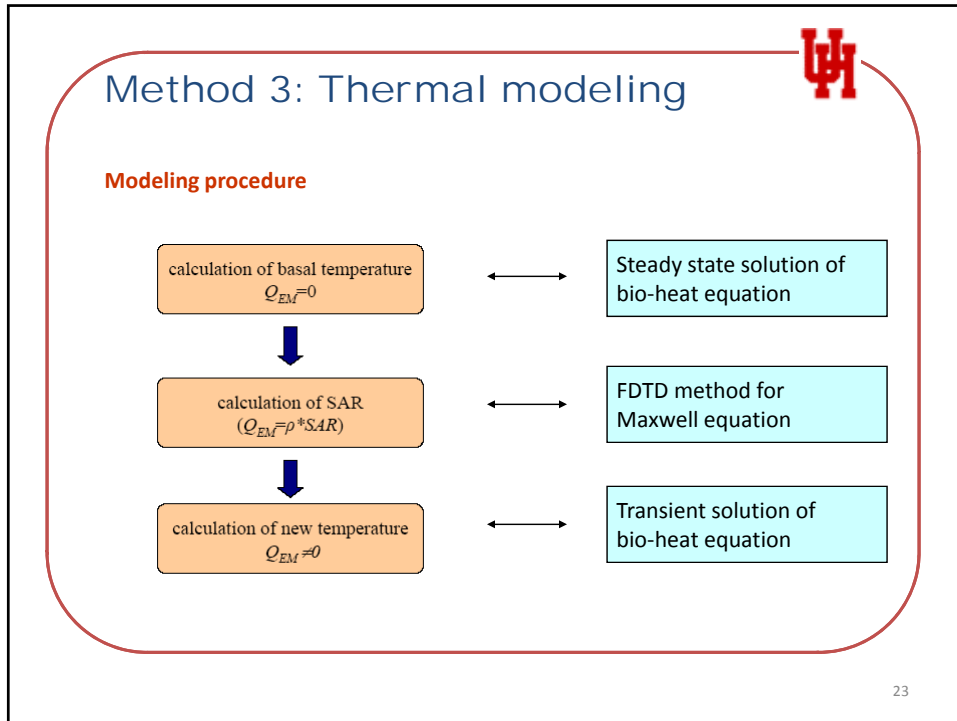
$Q_{EM} = \rho \text{SAR} \leftrightarrow$ from FDTD calculation


Boundary condition:

$$K \frac{\partial T}{\partial n} = -H_a (T - T_a)$$

Symbol	Physical Property	Units
T	Temperature	$^{\circ}\text{C}$
t	continuous time	s
n	surface normal	-
ρ	mass density	$\left[\frac{\text{kg}}{\text{m}^3} \right]$
C	specific heat	$\left[\frac{\text{J}}{\text{kg}^{\circ}\text{C}} \right]$
K	thermal conductivity	$\left[\frac{\text{J}}{\text{m}^2 \text{s}^{\circ}\text{C}} \right]$
H_a	convective transfer constant (for environmental ambient temperature)	$\left[\frac{\text{W}}{\text{m}^2 \text{s}^{\circ}\text{C}} \right]$
A_0	basal metabolic rate	$\left[\frac{\text{J}}{\text{m}^3 \text{s}} \right]$
B	blood perfusion constant	$\left[\frac{\text{m}^3}{\text{m}^3 \text{s}^{\circ}\text{C}} \right]$
m_b	blood mass flow rate	$\left[\frac{\text{m}^3}{\text{s kg}} \right]$
T_b	blood temperature (constant)	$^{\circ}\text{C}$
T_a	environment ambient temperature (constant)	$^{\circ}\text{C}$


22





Method 4: Equivalent source

Types of walk-through metal detector



A head-to-toe uniform detection field

~~coil configurations~~

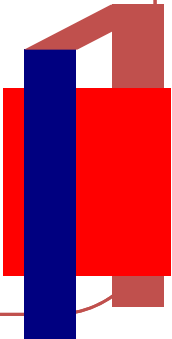
~~operational modes~~


Alternative Choice: Measure the magnetic field at a few planes

Method 1. X-ray the walk-through detector

Method 2. Interpolation of the measured field


Method 3. Equivalent source modeling





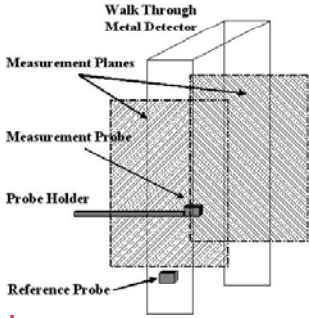
Pinpoint Detection with DSP Chip

25



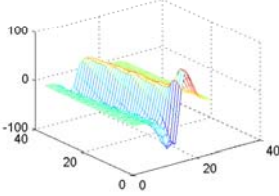
Method 4: Equivalent source

Illustration of magnetic field measurement

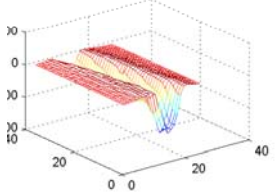


Each plane has a size of 120 cm in the horizontal direction and 180 cm in the vertical direction.

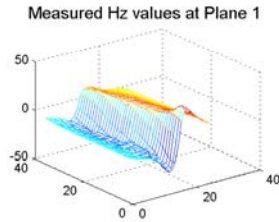
Measured Hx values at Plane 1



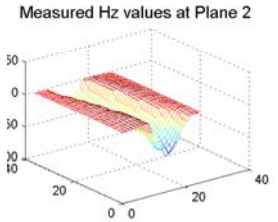
Measured Hx values at Plane 2




Measured Hz values at Plane 1



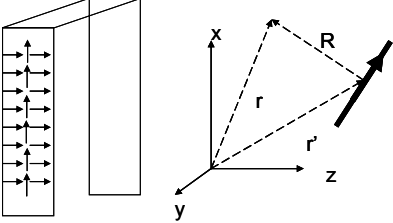
Measured Hz values at Plane 2





Method 4: Equivalent source

Equivalent source discretization and the coordinate system



This equivalent may not be the exact coil configurations but it can produce the same magnetic fields as that of the real coil configuration

Biot-Savart law

$$\vec{H} = \frac{1}{\mu} \vec{B} = \nabla \times \vec{A} = \int \frac{I(\vec{r}') d\vec{l}' \times \vec{R}}{4\pi |\vec{R}|^3}$$


Equivalent current distribution

H_x	[0	...	m_{xy}	...	m_{xz}]	J_x
...	
H_y	[m_{yx}	...	0	...	m_{yz}]	J_y
...	
H_z	[m_{zx}	...	m_{zy}	...	0]	J_z

Measured data

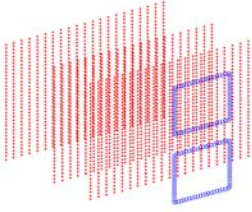
least square method

27

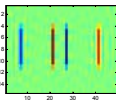


Method 4: Equivalent source

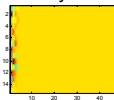
A numerical validation experiment
(magnetic fields generated by the two loop coils)



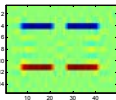
I_x



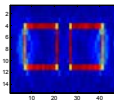
I_y



I_z



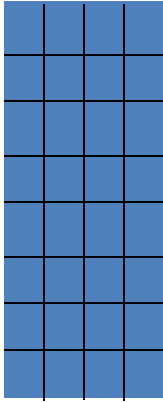
I_m



Method 4: Equivalent source

Equivalent source plane

1. Size
2. Mesh density

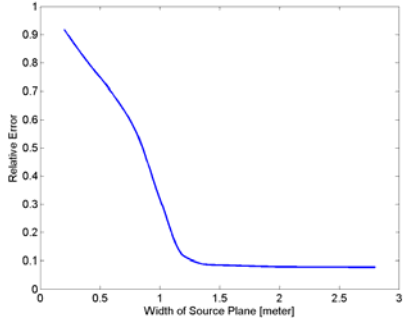


29

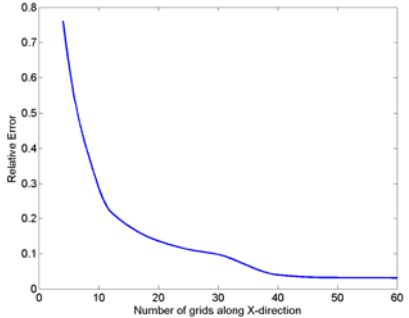
Method 4: Equivalent source

Convergence analysis

$$relative\ error = \frac{\sum |H_{simulated} - H_{measured}|}{\sum |H_{measured}|}$$



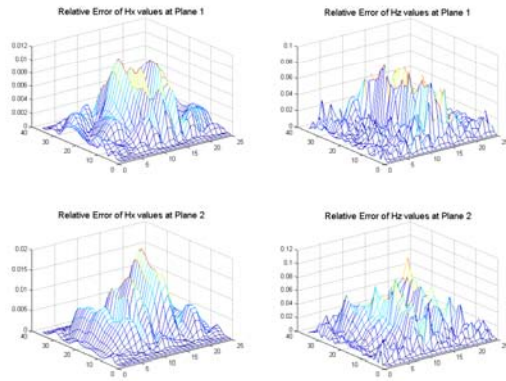
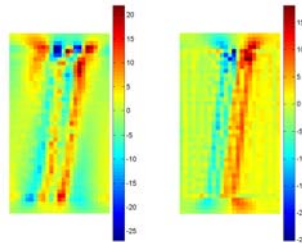
Width of Source Plane [meter]	Relative Error
0.25	0.9
0.5	0.7
0.75	0.55
1.0	0.4
1.25	0.1
1.5	0.1
2.0	0.1
2.5	0.1
3.0	0.1



Number of grids along X-direction	Relative Error
5	0.75
10	0.25
20	0.15
30	0.1
40	0.05
50	0.05
60	0.05

30


Method 4: Equivalent source



Applications




- Pregnant woman exposed to walk-through metal detector
- Pregnant woman under exposure to magnetic resonance imaging
- Safety evaluation of metallic implants in magnetic resonance imaging
- Interactions between medical implants and vehicular mounted antennas




Application 2: Safety assessment for WTMD

Safety evaluation of walk-through metal detectors



- Walk-through metal detectors are an important part of airport security systems
- Metal detectors use the electromagnetic signal variations as a means to detect metal objects
- Standard was developed based on male models, no safety assessment was performed for pregnant women
- Induced current strength should be used for emission safety assessment (hard to directly measure the induced current strength within human subjects)


33




Application 2: Safety assessment for WTMD

Develop a procedure that can be used towards accurate safety assessments for walk through metal detector electromagnetic emission

Measurement of magnetic fields



Equivalent source



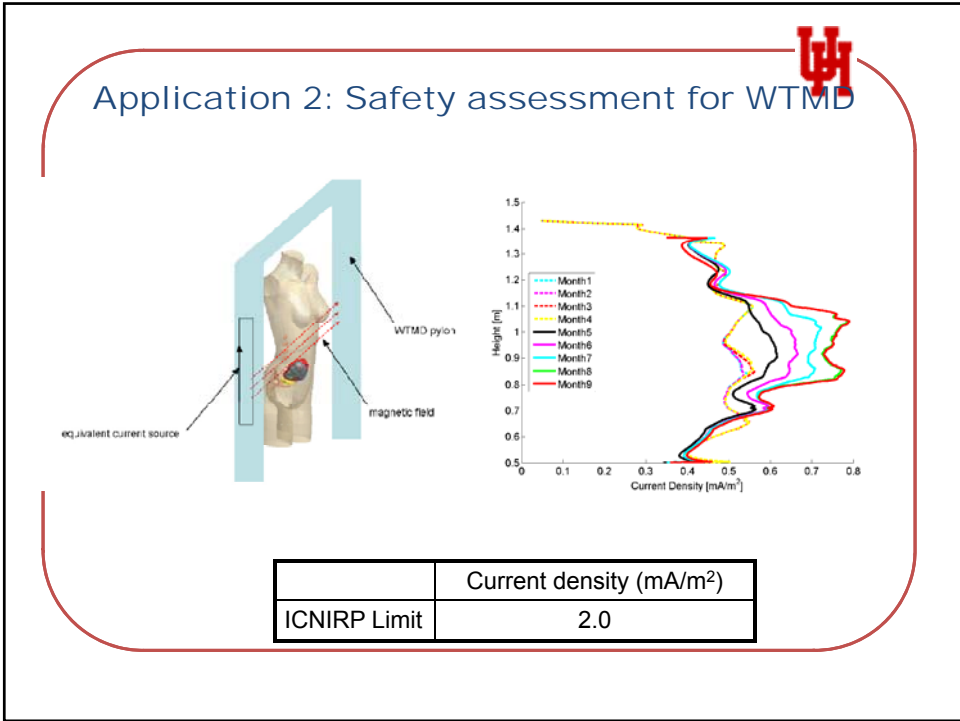
Evaluate induced currents (impedance method)

Represent the original walk-through metal detector electromagnetic emission

Able to calculate the magnetic field distribution at any points within the human subjects

Extreme low frequency modeling

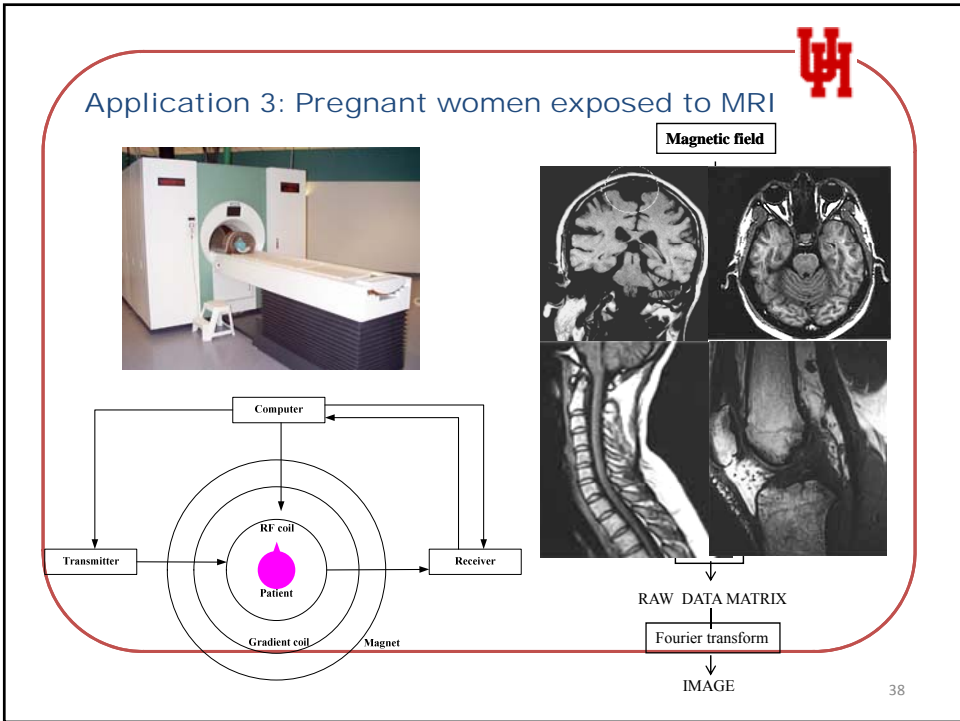
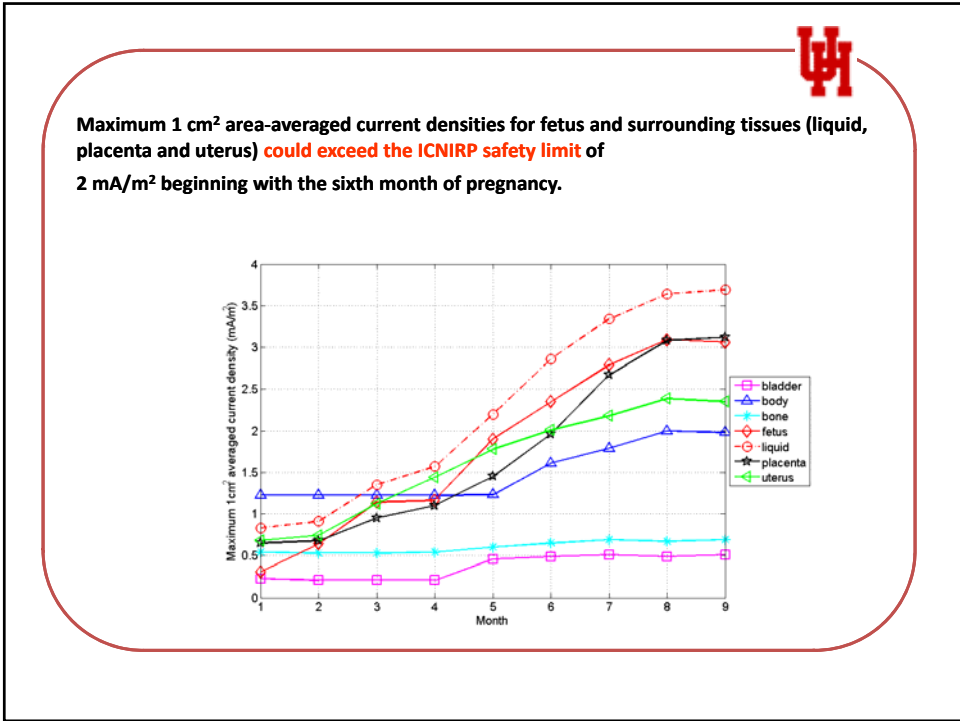
34



Application 2: Safety assessment for WTMD


J: induced current density (mA/m²)
E: Induced electric field (mV/m)

		Month1		Month2		Month3		Month4		Month5		Month6		Month7		Month8		Month9	
		J	E	J	E	J	E	J	E	J	E	J	E	J	E	J	E	J	E
bladder	Tissue-averaged	0.18	0.88	0.17	0.82	0.17	0.84	0.17	0.83	0.45	2.15	0.5	2.41	0.54	2.59	0.55	2.63	0.56	2.69
	Maximum (1cm ²)	0.23	1.13	0.21	0.99	0.21	1.02	0.21	1.01	0.46	2.21	0.49	2.35	0.51	2.44	0.49	2.37	0.51	2.44
body	Tissue-averaged	0.51	2.24	0.51	2.24	0.52	2.24	0.52	2.25	0.53	2.31	0.56	2.44	0.58	2.53	0.58	2.54	0.58	2.54
	Maximum (1cm ²)	1.22	5.29	1.22	5.29	1.22	5.29	1.22	5.29	1.23	5.34	1.61	7.01	1.79	7.78	2	8.7	1.98	8.59
bone	Tissue-averaged	0.12	5.76	0.11	5.56	0.12	5.77	0.11	5.65	0.2	9.79	0.21	10.36	0.22	11.08	0.23	11.37	0.23	11.51
	Maximum (1cm ²)	0.54	27	0.53	26.26	0.53	26.27	0.54	26.89	0.6	29.58	0.65	32.42	0.69	34.17	0.67	33.3	0.69	34.01
fetus	Tissue-averaged	0.34	1.84	0.31	1.68	0.35	1.9	0.32	1.73	0.29	1.57	0.33	1.79	0.36	1.93	0.38	2.03	0.38	2.02
	Maximum (1cm ²)	0.31	1.65	0.64	3.42	1.14	6.1	1.16	6.22	1.9	10.23	2.35	12.65	2.79	15.01	3.09	16.61	3.06	16.45
liquid	Tissue-averaged	0.87	0.58	0.9	0.6	1.08	0.72	1.27	0.84	1.44	0.96	1.63	1.09	1.83	1.22	2.05	1.37	2.05	1.37
	Maximum (1cm ²)	0.83	0.55	0.91	0.61	1.35	0.9	1.57	1.04	2.2	1.47	2.86	1.91	3.34	2.23	3.64	2.42	3.69	2.46
placenta	Tissue-averaged	0.41	0.59	0.48	0.69	0.56	0.8	0.65	0.92	0.62	0.89	0.69	0.98	0.77	1.1	0.85	1.22	0.85	1.22
	Maximum (1cm ²)	0.65	0.92	0.68	0.97	0.95	1.35	1.1	1.58	1.45	2.07	1.96	2.79	2.67	3.81	3.08	4.4	3.12	4.46
uterus	Tissue-averaged	0.54	1.1	0.54	1.09	0.64	1.3	0.64	1.31	0.72	1.47	0.84	1.72	0.99	2.03	1.12	2.28	1.12	2.28
	Maximum (1cm ²)	0.68	1.38	0.74	1.52	1.12	2.28	1.44	2.94	1.78	3.63	2.01	4.11	2.18	4.44	2.39	4.87	2.35	4.79





UP

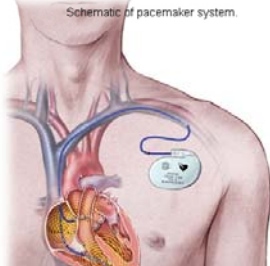
Application 3: Pregnant women exposed to MRI



Second Degree Skin Burn







Schematic of pacemaker system.

UP

Application 3: Pregnant women exposed to MRI

Methodology

Develop simulation models including human body and MRI RF coil

↓

Calculate EM fields inside exposed human subjects

↔

Solve Maxwell's equation by means of finite-difference time domain method

↓

Compute temperature rises of tissues

↔

Solve Bio-heat equation:

$$C\rho \frac{\partial T}{\partial t} = K\nabla^2 T + A_0 - B(T - T_b) + \text{SAR}$$

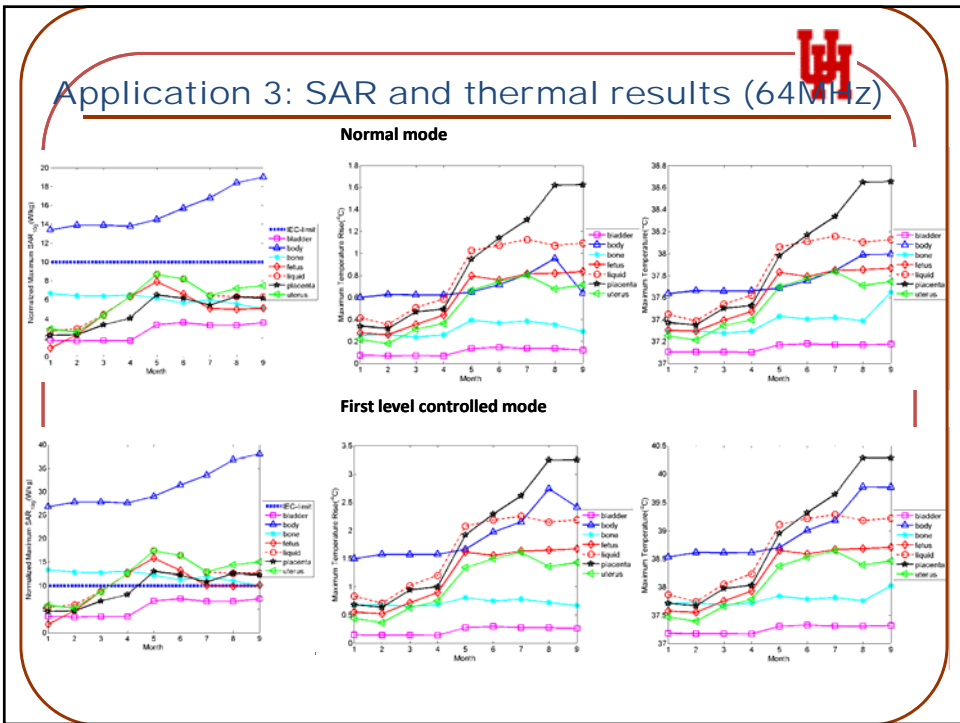
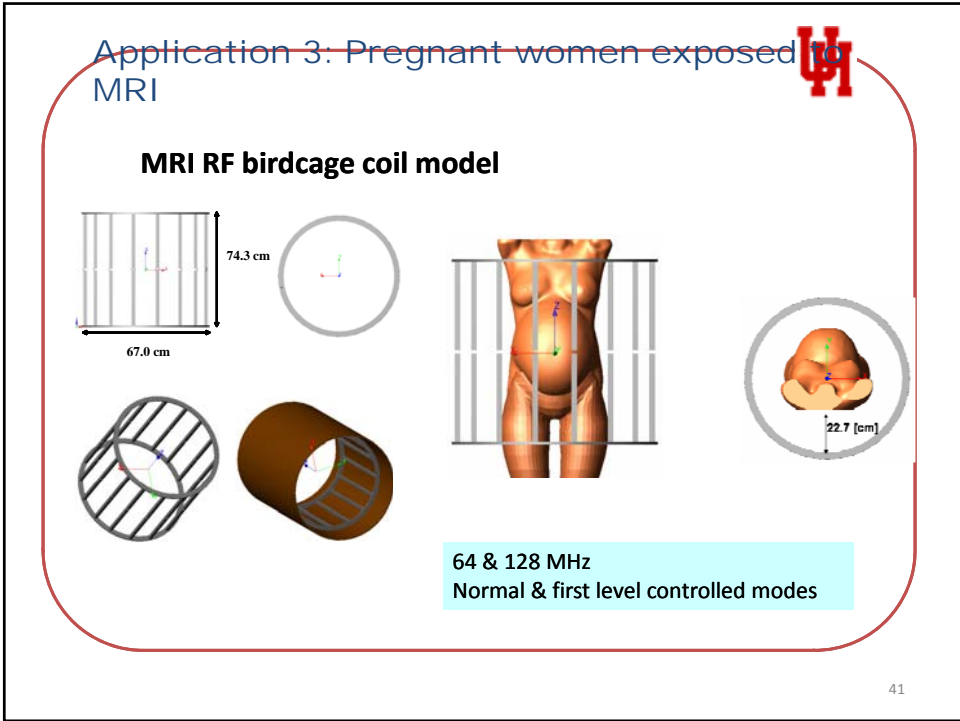
↓

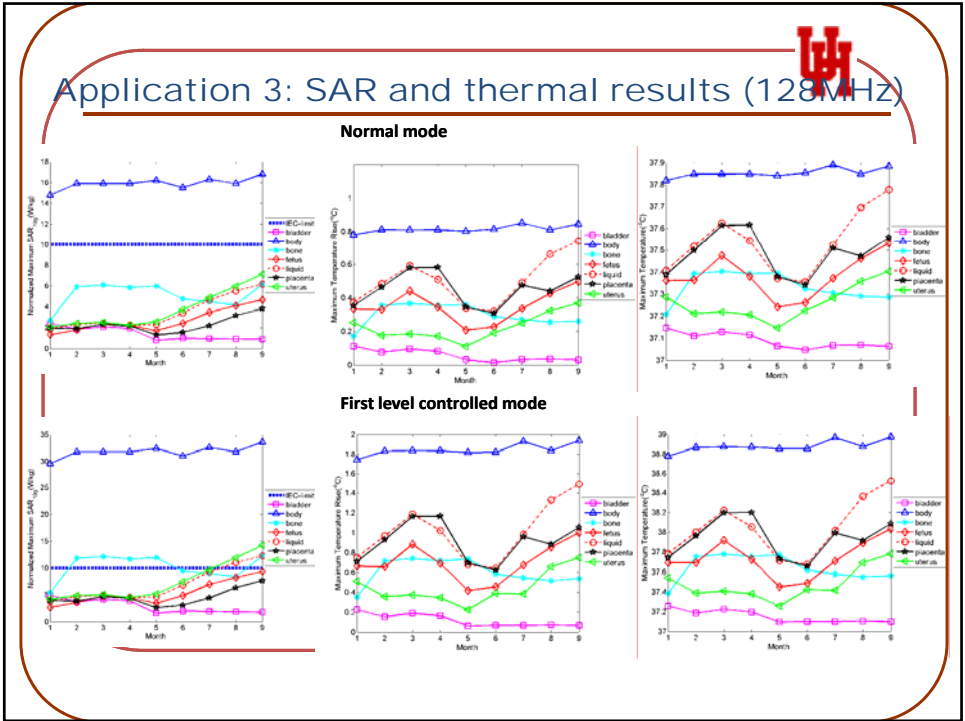
Normalize the simulated data and compare them with the IEC safety limit.

$$\text{SAR} = \frac{\sigma}{2\rho} |E|^2$$

MRI Operating mode	Whole body SAR (W/kg)	Local SAR _{10g} - Body (W/kg)	Maximum temperature (°C)
Normal	2	10	39.0
First level controlled	4	10	39.0

40



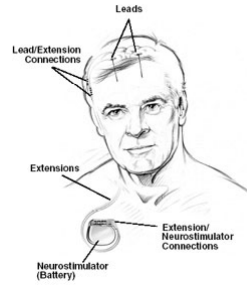
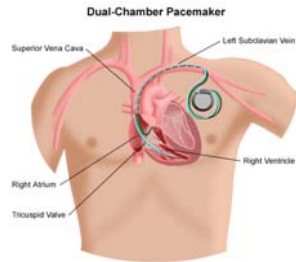


Fetus		64 MHz		128 MHz	
		Normal Mode	First level controlled mode	Normal Mode	First level controlled mode
Month 1-4	SAR limit	Not exceed	Not exceed	Not exceed	Not exceed
	Temperature limit	Not exceed	Not exceed	Not exceed	Not exceed
Month 5-9	SAR limit	Not exceed	Exceed	Not exceed	Not exceed
	Temperature limit	Not exceed	Not exceed	Not exceed	Not exceed

Based on the results of this study, we recommend **not performing MRI procedures on pregnant women using the first level controlled mode**. These results can also be used towards developing safety standards for pregnant woman undergoing an MRI.

SAR and temperature rise distributions are **quite different** at the two MRI operating frequencies. Such variation is caused by the different electric field distributions generated by MRI coils at these two frequencies and it is also related to the difference in dielectric parameters at these two frequencies.

Application 4: Safety of metallic implants within MRI coil

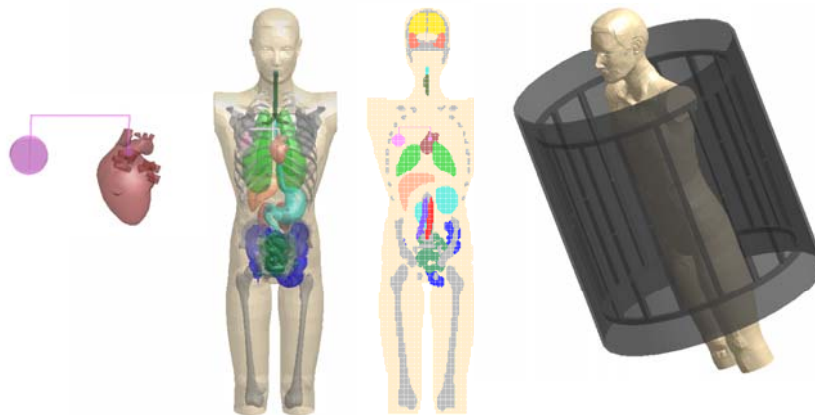


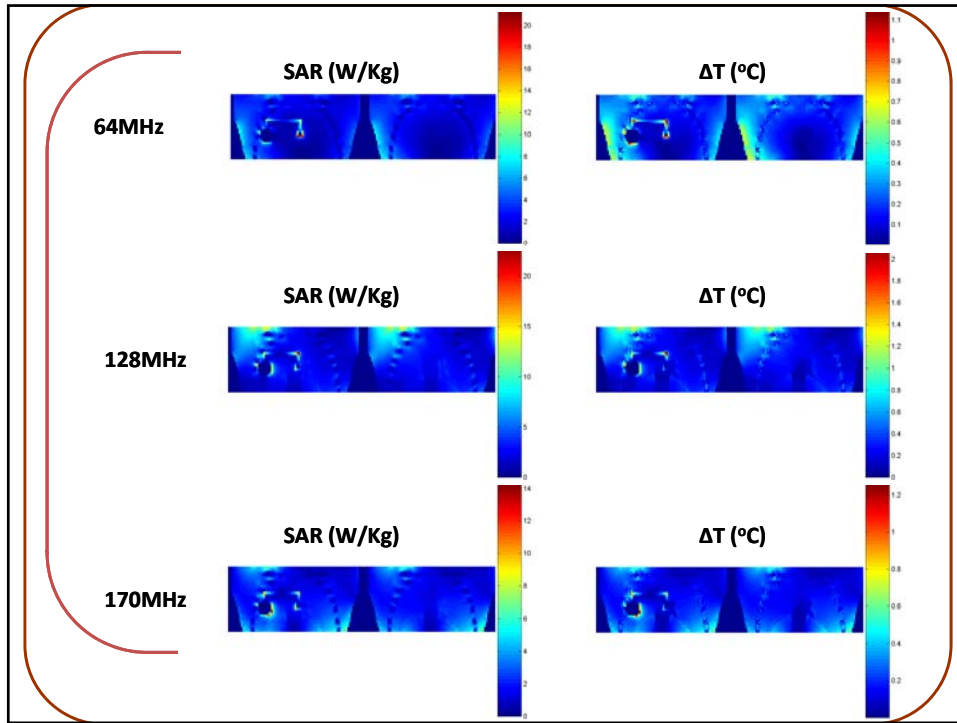
On May 10, 2005, in response to several reports of serious injuries from medical facilities around the country, the FDA issued a Public Health Notification reminding all medical personnel of the importance of properly screening patients for implanted neurological stimulators before administering an MRI.


Application 4: Safety of metallic implants within MRI coil




Simulation model






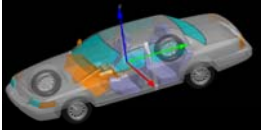


	Maximum SAR (W/kg)						Maximum temperature rise (oC)						Maximum temperature (oC)					
	64MHz		128MHz		170MHz		64MHz		128MHz		170MHz		64MHz		128MHz		170MHz	
	With	W/o	With	W/o	With	W/o	With	W/o	With	W/o	With	W/o	With	W/o	With	W/o	With	W/o
blood	6.47	6.39	14.86	15.07	9.01	8.7	0.91	0.9	1.72	1.69	1	0.98	37.91	37.9	38.72	38.69	38	37.98
bone	2.4	2.37	2.9	2.93	3.25	3.25	2.49	2.48	2.69	2.75	2.1	2.11	39.67	39.66	39.88	39.94	39.29	39.29
brain	0.19	0.18	5.08	5.1	4.51	4.55	0.02	0.02	0.55	0.55	0.46	0.46	37.31	37.31	37.85	37.84	37.75	37.76
eye	0.05	0.04	1.01	1.01	2.51	2.52	0.01	0.01	0.13	0.13	0.33	0.33	37.01	37.01	37.13	37.13	37.33	37.33
heart	6.49	0.95	4.44	3.25	3.21	2.41	1	0.05	0.66	0.19	0.48	0.13	38.29	37.35	37.96	37.48	37.78	37.82
intestine large	19.83	22.02	11.88	11.92	9.33	9.35	2.06	2.04	1.15	1.14	1.03	1.03	37.5	37.5	37.45	37.45	37.64	37.64
intestine small	10.97	10.86	9.44	9.48	10.11	10.13	1.71	1.7	1.18	1.17	0.97	0.96	37.61	37.62	37.4	37.4	37.79	37.79
kidney	3.11	3.08	2.54	2.57	5.48	5.52	0.21	0.21	0.15	0.15	0.34	0.35	38.95	38.94	38.28	38.27	38.32	38.32
liver	5.55	5.6	1.71	1.74	7.9	7.95	0.32	0.32	0.1	0.1	0.49	0.5	38.44	38.49	38.72	38.22	38.76	38.76
lung	8.44	8.77	7.38	7.51	11.31	11.43	1.15	1.19	1.42	0.92	1.47	1.47	39.41	39.4	39.41	38.95	38.7	38.7
muscle	24.53	24.25	19.02	19.16	15.98	16.08	2.88	2.86	2.16	1.87	1.74	1.74	39	38.99	38.47	38.47	38.26	38.26
Stomach	4.52	4.55	10.5	10.61	12.96	12.98	0.6	0.62	1.2	1.16	1.49	1.49	37.89	37.9	38.49	38.44	38.77	38.77
windpipe	3.27	3.46	6.94	6.98	2.86	2.84	0.49	0.51	1	0.98	0.4	0.38	37.6	37.62	38.11	38.09	37.51	37.49

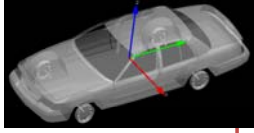





A typical police car (Ford Crown Victoria)



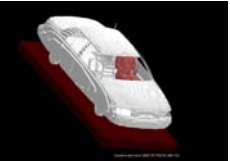
CAD model of the car



Car with metal parts only
According to IEEE P1528.2



Bystander




Passenger

Ground is 30cm thick slab, with relative permittivity 8 and conductance 0.01 S/m, extend 10cm in x and y Direction beyond the car/bystander.

According to IEEE 1528.3 On the Ground Modeling Implementation

51



Antenna

- 1/4 30 MHz
- 1/4 75 MHz
- 1/4 150 MHz
- 1/4 450 MHz
- 1/4 900 MHz
- 5/8 150 MHz
- 5/8 450 MHz
- 5/8 900 MHz

d-distance

- 20cm away
- 100cm away

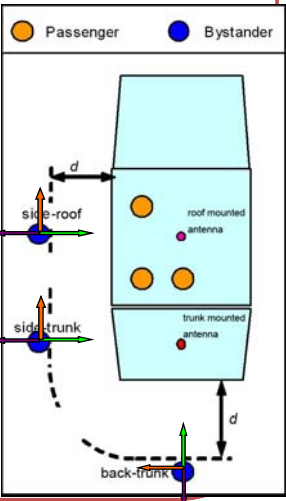
Three facing direction:

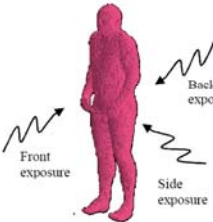
- ↑ Bystander model 1 --> facing the car
- ↑ Bystander model 2 --> facing front
- ↑ Bystander model 3 --> face off the car

Four seat modeling:


- Passenger no additional parts
- Passenger model 1 --> with metal seat
- Passenger model 2 --> with spring coils
- Passenger model 3 --> with both seat & coils

● Passenger
 ● Bystander



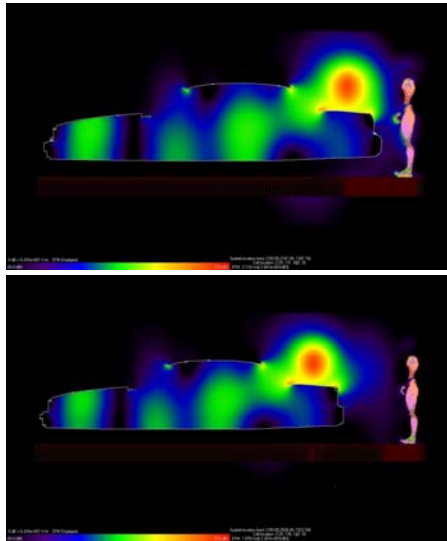
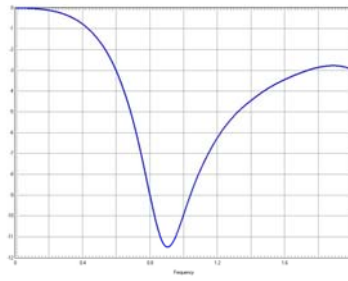


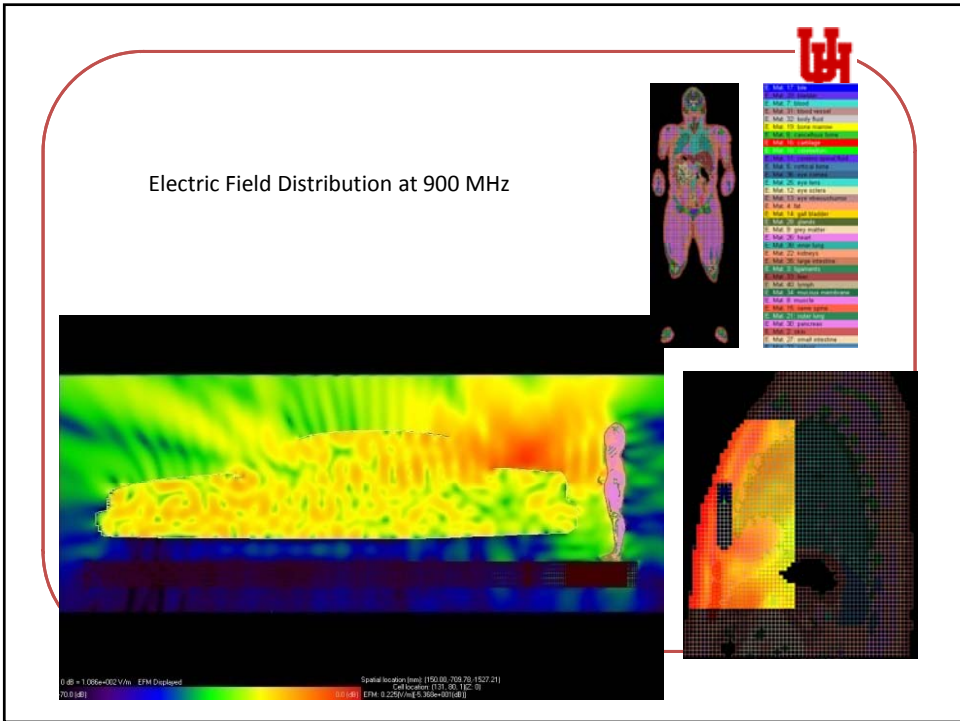
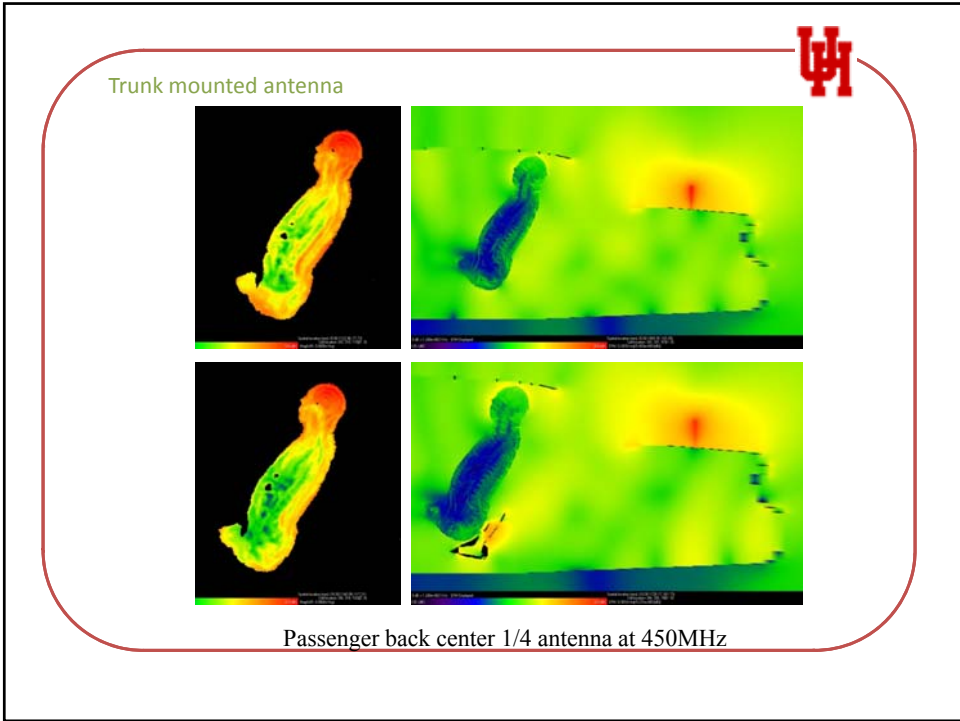
Front exposure
Back exposure
Side exposure





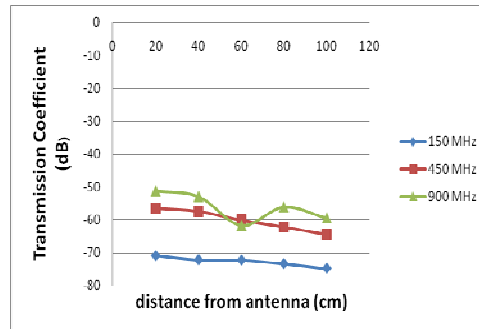
Design of Implantable Antenna







	SAR with Device (W/kg)	SAR W/O Device (W/kg)
150 MHz	0.0028	0.0020
450 MHz	0.0041	0.0034
900 MHz	0.0077	0.0067

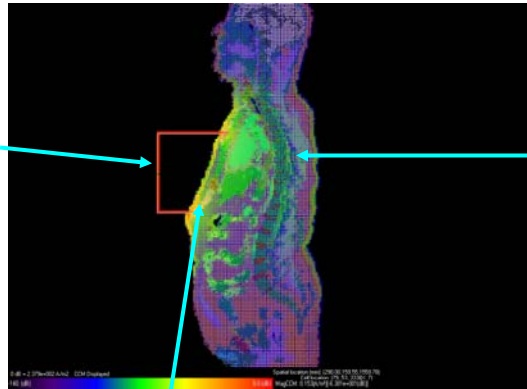


Modeling:

Darts at front, induced current within human models



Modeling of taser darts (5 mm into human model)



human model

different color corresponds induced current strength. For example, red color corresponds to large current strength

